Cytoplasmic Domain Filter Function in the Mechanosensitive Channel of Small Conductance

Ramya Gamini,[†‡] Marcos Sotomayor,[§] Christophe Chipot,[†¶] and Klaus Schulten[†‡*]

[†]Beckman Institute and [‡]Center for Biophysics and Computational Biology, University of Illinois at Urbana-Champaign, Champaign, Illinois; [§]Howard Hughes Medical Institute and Department of Neurobiology, Harvard Medical School, Boston, Massachusetts; and [¶]Équipe de Dynamique des Assemblages Membranaires, Centre National de la Recherche Scientifique UMR 7565, Nancy Université, Vandœuvre-lès-Nancy, France

ABSTRACT Mechanosensitive channels, inner membrane proteins of bacteria, open and close in response to mechanical stimuli such as changes in membrane tension during osmotic stress. In bacteria, these channels act as safety valves preventing cell lysis upon hypoosmotic cell swelling: the channels open under membrane tension to release osmolytes along with water. The mechanosensitive channel of small conductance, MscS, consists, in addition to the transmembrane channel, of a large cytoplasmic domain (CD) that features a balloon-like, water filled chamber opening to the cytoplasm through seven side pores and a small distal pore. The CD is apparently a molecular sieve covering the channel that optimizes loss of osmolytes during osmoadaptation. We employ diffusion theory and molecular dynamics simulations to explore the transport kinetics of Glu^- and K^+ as representative osmolytes. We suggest that the CD indeed acts as a filter that actually balances passage of Glu^- and K^+, and possibly other positive and negative osmolytes, to yield a largely neutral efflux and, thereby, reduce cell depolarization in the open state and conserve to a large degree the essential metabolite Glu^-.

INTRODUCTION

MscS, the mechanosensitive channel of small conductance, belongs to a family of pressure-sensitive channels that play a major role in osmoadaptation of bacterial cells (1,2). Bacteria experience changes in membrane tension as a consequence of water influx and efflux induced by an imbalance of osmolytes between intra- and extracellular spaces. The channels perceive membrane tension resulting from swelling and function as safety valves to alleviate cell turgor by releasing osmolytes along with water and, thereby, prevent cell lysis (3). The MscS channel opens at slight pressure differences of tens of mmHg, assuming then a conductance of 1 nS.

Bacteria feature three functionally similar mechanosensitive channels: MscM (M for mini), MscS (S for small), and MscL (L for large). These channels respond in a graded manner to relieve the cell from osmotic stress (4,5). MscM opens most readily in response to membrane tension, assuming then a conductance of 0.1–0.3 nS. MscL opens in response to pressure changes approaching the cell lytic limit, namely $\Delta p < -40$ mmHg (-40 torr), assuming a conductance of 3 nS (6); MscL opens only as a last resort, i.e., it functions as an emergency valve to release all contents, even proteins, to help the cell escape imminent cell lysis (3,5,7,8). Experiments have provided a great deal of phenotypic evidence to suggest the physiological role of these channels in osmosensing and adaption during osmotic shock.

MscS is a homoheptameric complex, each monomer (P1–P7) of the *Escherichia coli* channel consisting of 286 amino acids. Two crystal structures of *E. coli* MscS have been determined, one of the wild-type (PDB: 2OAU) with MscS in a putative closed state (9,10) and the other of a mutant (A106V, PDB: 2VV5) with MscS trapped in an open state (11). The channel subunits have two distinct domains, a transmembrane (TM) domain and a cytoplasmic domain (CD) (Fig. 1, *a* and *b*). Each TM domain comprises three α-helices labeled TM1, TM2, and TM3. The seven subunits form a central TM pore made of 21 helices that sense tension and open and close the channel as discussed in the literature (9,10,12–20).

The two crystal structures of MscS (9–11), although representing different putative states of the TM domain, depict the same architecture for MscS' large cytoplasmic domain (Fig. 1 *b*). The CD comprises ~65% of the total mass of the protein and is a conserved structural feature in the MscS family whose function remains unclear. The CD (shown in Movie S1 in the Supporting Material) is mainly composed of β-sheets that form a balloon-shaped, water-filled chamber with a diameter of ~80 Å. The CD has seven distinct, roughly hourglass-shaped side openings, each ~7 Å wide in the middle, formed between adjacent MscS subunits and has a single narrow axial opening distal to the pore. The side openings (Fig. 1 *c*) are lined by side chains that are basic, acidic, polar, and nonpolar, thus suggesting only weak selectivity, if any at all, in regard to solutes allowed to pass through. In accordance with this feature, both K^+ and Cl^- have been observed in simulations to pass through the openings (13,15). The narrow distal opening has its interior lined with hydrophobic residues which prevent easy passage of hydrated solutes, such that this opening appears to be effectively closed.

Submitted December 21, 2010, and accepted for publication May 16, 2011.

*Correspondence: kschulte@ks.uiuc.edu

Editor: Scott Feller.

© 2011 by the Biophysical Society

0006-3495/11/07/0080/10 $2.00

doi: 10.1016/j.bpj.2011.05.042

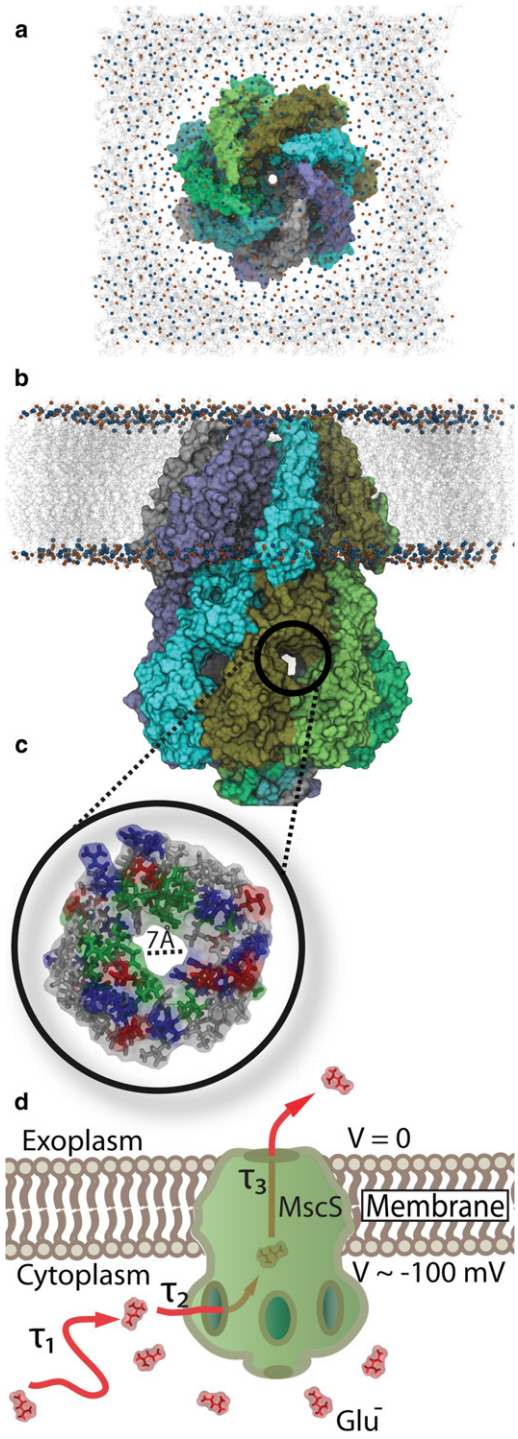

FIGURE 1 Placement of MscS in the cell membrane. (*a* and *b*) Top and side views of the homoheptameric MscS (PDB:2OAU), respectively. The latter view distinguishes clearly the transmembrane and the cytoplasmic domains. The cytoplasmic domain contains seven equal openings on its side, one being clearly visible and enlarged, exhibiting the 7 Å opening in panel *c*. Colors distinguish the seven MscS subunits. (*c*) (*Circular inset*) View of the side opening showing MscS as a transparent surface with side groups lining the opening in licorice representation (colors *gray*, *green*, *red*, and *blue* denoting nonpolar, polar, negative, and positive side groups, respectively). (*d*) Schematic illustration of MscS and the passage of cellular material from the cytoplasm to the extracellular space upon opening of the channel due to an osmotic pressure difference. A negative intracellular voltage drives negative ions, e.g., the osmolyte Glu^-, out of the cell. MscS combines a transmembrane domain with a mechanosensitive channel and a large cytoplasmic domain of unclear function. Here the possible function of the cytoplasmic domain as a filter is investigated. An intracellular solute would leave the cell in three steps: 1), diffusion toward the cytoplasmic domain; 2), translocation through openings in this domain; and 3), translocation through the transmembrane channel. The values τ_1, τ_2, and τ_3 denote the durations of the respective steps. Movie S1 provides a close-up three-dimensional view of MscS and, in particular, of the CD and its openings.

The CD side openings are the only gateway for water and cytoplasmic solutes to reach the cell exterior (see Fig. S1 in the Supporting Material). Translocation of solutes involves three steps as shown in Fig. 1 *d*: 1), diffusion of solutes toward the CD requiring a time τ_1 to find a side opening; 2), passage of solutes through an opening requiring a time τ_2; and finally 3), translocation through the TM pore to the cell exterior requiring a time τ_3.

The present study focuses on function and mechanism of the MscS CD. Various investigations suggest the CD to play a role in channel gating (21–25) and MscS conductivity (17). Deletion studies suggest the domain to be required for gating and stability of the channel (22,26). Here we consider, however, another likely function of the CD, namely that of a sieve that regulates the efflux of solutes valuable to the cell. Such function is consistent with the observation that MscS with a largely deleted CD remains physiologically functional (26), the respective cells being, however, less viable under high salt conditions (17). MscS without its sieve could still protect the cell from osmotic shock by opening and closing its TM domain, but would do this at a higher cost to the cell as it would spill too much of its valuable content during osmoadaptation. Furthermore, the CD appears to be specifically designed to prevent dominant efflux of negative ions, e.g., Glu^-, an efflux which is favored by the cellular potential, and instead appears to maintain, by mixing equal amounts of Glu^- and K^+ ions or other anions and cations, neutral efflux that conserves the cellular potential.

In our study of MscS' filter and mixing function, we select two osmolytes for particular attention, namely, Glu^- and K^+. We consider Glu^- and K^+ as exemplary cytoplasmic solutes that shed light on MscS' function in general due to their high concentration in *E. coli* cells. Our approach involves mathematical and computational modeling. We present a mathematical description of the diffusion-controlled approach of Glu^- and K^+ to the MscS CD and to the side opening, obtaining an estimate for the time τ_1 (see Fig. 1 *d*). We then describe computationally the transport of Glu^- through a CD opening providing an estimate for the time τ_2, and through an account of the transmembrane potential, we estimate the channel passage time τ_3. Values τ_1, τ_2, and τ_3 are also estimated for K^+. The calculations lead us to the overall conclusion that the CD of MscS

balances passage of Glu^-, K^+, and other osmolytes. The key finding is that MscS achieves its functionality seemingly without its side openings getting clogged and with minimizing loss of cell polarization.

METHODS

Systems modeled

The MscS cytoplasmic domain (CD) was modeled starting from the full atomic structure obtained at a resolution of 3.9 Å from x-ray crystallography (PDB 2OAU) (9,10). We note here that the crystal structure lacks a six-amino-acid segment at the C-terminus which has zero net charge; we do not model this segment in our system. The CD of the wild-type protein modeled here is essentially similar to that found in the putative open mutant A106V (11). The CD construct was obtained by removing the N-terminal transmembrane residues 27–112; the resulting N-terminus was modified with *N*-acetyl using the PSFGen plugin of VMD (27) to have an uncharged N-terminus. The plugin also placed the missing hydrogen atoms into the structure. The CD was solvated using the Solvate plugin of VMD to add 13 Å of water padding in each direction. In order to compute the intrinsic electrostatics of the CD, the solvated system of the MscS CD, which has an overall charge of $-7.0e$, was neutralized by placing into the simulated volume seven K^+ counterions using the cIonize plugin of VMD.

The resulting system of the CD in a water box, SimA, had 128,390 atoms (in a 10.8 nm × 11.1 nm × 10.3 nm volume). System SimB was modeled adding K^+ and Glu^- ions to the solvated system at random positions using the VMD ionize plugin such that the neutralized system contained 200 mM KGlu. This concentration is within the typical KGlu range found in bacterial cells (28). We modeled free glutamate molecules as zwitterions carrying a net $-1.0e$ charge due to its side chain. The resulting setup had 123,462 atoms (in a 10.8 nm × 10.8 nm × 10.1 nm volume). In all simulations, constraints were imposed on the C_α atoms of residues 274 and 120 of all subunits, P1–P7, to prevent the domain from drifting during simulations; the constraint assumed for this purpose was harmonic with a spring constant of 1.0 kcal mol^{-1} $Å^{-2}$. Molecular dynamics simulations were performed as described in the Supporting Material.

Electrostatic potential map

In order to evaluate the average intrinsic electrostatic map of the CD, 14.3 ns equilibrium simulations of the SimA setup in the NVT ensemble were performed at zero bias potential. The VMD PMEpot plugin (29,30), which uses the particle-mesh Ewald method (31), was employed to compute the electrostatic potential map for every frame (2 ps). This electrostatic potential was evaluated using a three-dimensional grid of 108 × 112 × 108 points (which ensured at least one grid point per Å in each direction), and was averaged over entire trajectories including all atoms of the system.

Potential of mean force

The potential of mean force (PMF) of glutamate (Glu^-) translocating through the MscS side opening was evaluated from equilibrium adaptive biasing force (ABF) simulations (32–36). The ABF method has been widely used in conjunction with molecular dynamics simulation for the evaluation of the PMF of many biologically and chemically interesting systems (35,37–39). In ABF simulations, the system is subject to a continuously updated biasing force designed to eventually remove all energetic barriers along a chosen coordinate and, thus, allow free diffusion of the system along that coordinate. Once the calculation converges, a PMF along the chosen coordinate is obtained through thermodynamic integration (34). The details of the calculations are described in the Supporting Material. Movie S2, a visualization of the ABF trajectory, is also provided there.

Rate of diffusion-controlled reaction

Here we derive, following Schulten and Schulten (40), the rate of diffusion-controlled approach of Glu^- in the cellular cytoplasm to the CD followed by successful entry into one of the side openings of the CD. The derivation is provided for the sake of completeness, as the one in Schulten and Schulten (40) is extremely brief. The theory of diffusion-controlled reactions is due to Debye (41) and Eigen (42).

As not every diffusive encounter between solute and CD leads to entering of an opening, the diffusive encounter is characterized as a reaction with a finite, in fact, small, reaction probability, controlled through the parameter w employed below, $w = 0$, corresponding to no reaction and $w \to \infty$ corresponding to every encounter leading to a reaction. We approximate the CD as a sphere as we are only interested in a rough estimate of the diffusion rate.

The diffusion-reaction process (reaction = entrance into an opening), described through the probability distribution $p(\vec{r},t)$ for finding Glu^- at position $\vec{r}$ at time t near the CD, is governed by the Smoluchowski equation (43)

$$\partial_t p(\vec{r},t) \;=\; \nabla \cdot D(\vec{r})[\nabla - \beta\vec{F}(\vec{r})]p(\vec{r},t). \tag{1}$$

Here $\vec{F}(\vec{r})$ is the force acting on the solute and $D(\vec{r})$ is the local diffusion coefficient. The solution of Eq. 1 is subject to the boundary condition

$$\widehat{n}(\vec{r}) \cdot D(\vec{r})[\nabla - \beta\vec{F}(\vec{r})]p(\vec{r},t) \;=\; wp(\vec{r},t) \quad \text{at } |\vec{r}| \;=\; R_o \tag{2}$$

for some constant w that has been introduced above ($\widehat{n}(\vec{r})$ is the normal to the surface). Assuming that the concentration, c_S, of Glu^- in the cytoplasm at a far distance from the CD remains constant, i.e., each translocated Glu^-, upon reaction, is immediately replaced at a random location in the cytoplasm, one can assume that the solution of Eq. 1 is time-independent, such that the Smoluchowski equation becomes

$$\nabla \cdot D(\vec{r})[\nabla - \beta\vec{F}(\vec{r})]p(\vec{r}) \;=\; 0, \tag{3}$$

with the additional (Eq. 2 also holds) boundary condition

$$\lim_{|\vec{r}|\to\infty} p(\vec{r}) \;=\; c_S. \tag{4}$$

This approach describes well the initial phase of Glu^- depletion, when c_S is still at a maximum. The later phase of depletion of c_S around the CD would have to be described through a more cumbersome, time-dependent solution of Eq. 1. The occurrence of an entrance of the solute into a CD opening implies that a stationary current develops which describes the diffusive approach of Glu^-. We consider in the following the case that the interaction between CD and Glu^- is due to a Coulomb potential $U(r) = q_{CD}q_S/\varepsilon r$ (ε = dielectric constant), which depends solely on the distance $|\vec{r}|$ of Glu^- from the CD center. We also assume that the diffusion coefficient D depends solely on $|\vec{r}|$. The stationary Smoluchowski equation (Eq. 3) is then angle-independent and reads

$$r^2\partial_r r^{-2} D(r)[\partial_r - \beta F(r)]p(r) \;=\; 0 \tag{5}$$

to which is associated the radial current

$$J_{tot}(r) \;=\; 4\pi r^2 D(r)[\partial_r - \beta F(r)]p(r) \tag{6}$$

where we have integrated over all directions $\hat{r}$ obtaining the total current, J_{tot}, at radius r. Employing $F(r) = -\partial_r U(r)$, one can express Eq. 6 as

$$J_{tot}(r) \;=\; 4\pi r^2 D(r)\exp[-\beta U(r)]\partial_r \exp[\beta U(r)]p(r). \tag{7}$$

However, according to Eq. 5 $J_{tot}(r)$ is independent of r. It must hold, in particular,

$$J_{tot}(R_o) \;=\; J_{tot}(r). \tag{8}$$

The boundary condition, from Eq. 2, together with Eq. 7, yields

$$4\pi R_o^2 w p(R_o) = 4\pi r^2 D(r)\exp[-\beta U(r)]\partial_r \exp[\beta U(r)]p(r). \quad (9)$$

This relationship, a first-order differential equation, allows one to determine $p(r)$.

For the evaluation of $p(r)$, we write Eq. 9 as

$$\partial_r\left[e^{\beta U(r)}p(r)\right] = \frac{R_o^2 w}{r^2 D(r)}p(R_o)e^{\beta U(r)}. \quad (10)$$

Integration $\int_r^\infty dr\cdots$ yields

$$p(\infty)e^{\beta U(\infty)} - p(r)e^{\beta U(r)} = R_o^2 w\, p(R_o)\int_r^\infty dr'\frac{e^{\beta U(r')}}{r'^2 D(r')} \quad (11)$$

or, using Eq. 4 and $U(\infty) = 0$,

$$p(r)e^{\beta U(r)} = c_S - R_o^2 w\, p(R_o)\int_r^\infty dr'\frac{e^{\beta U}(r')}{r'^2 D(r')}. \quad (12)$$

Evaluating this at $r = R_o$ and solving for $p(R_o)$ leads to

$$p(R_o) = \frac{c_S e^{-\beta U(R_o)}}{1 + R_o^2 w\, e^{-\beta U(R_o)}\int_{R_o}^\infty dr\, e^{\beta U(r)}/r^2 D(r)}. \quad (13)$$

We are presently interested in the rate at which the diffusive approach to the CD and entering into the CD openings proceeds. This rate is given by $J_{tot}(R_o) = 4\pi {R_o}^2 w\, p(R_o)$. Hence, we can state

$$\text{Rate} = \frac{4\pi R_o^2 w\, c_S\, e^{-\beta U(R_o)}}{1 + R_o^2 w\, e^{-\beta U(R_o)}\int_{R_o}^\infty dr\, e^{\beta U(r)}/r^2 D(r)}. \quad (14)$$

This expression is proportional to c_S, a dependence expected for the monomolecular reaction between solute and a single CD.

We define a corresponding, c_S-independent, rate constant k through

$$\text{Rate} = k(R_o, w)c_S \quad (15)$$

where we state explicitly the dependence of k on R_o and w. This rate constant is then, in the present case,

$$k(R_o, w) = \frac{4\pi}{\int_{R_o}^\infty dr\, \mathcal{R}(r) + e^{\beta U(R_o)}/R_o^2 w}. \quad (16)$$

Here, we defined

$$\mathcal{R}(r) = e^{\beta U(r)}/r^2 D(r). \quad (17)$$

We consider first the case of very ineffective reactions described by small w values. In this case, the time required for the diffusive encounter of solute and CD can become significantly shorter than the time for the local reaction to proceed, if it proceeds at all. In this case, it may hold that

$$\frac{e^{\beta U(R_o)}}{R_o^2 w} \gg \int_{R_o}^\infty dr\, \mathcal{R}(r) \quad (18)$$

and the reaction rate Eq. 16 becomes

$$k(R_o, w) = 4\pi R_o^2 w\, e^{-\beta U(R_o)}. \quad (19)$$

This expression conforms to the well-known Arrhenius law.

We want to apply Eqs. 16 and 17 to two cases—free diffusion ($U(r) \equiv 0$) and diffusion in a Coulomb potential ($U(r) = q_1 q_2/\varepsilon r$). We assume in both cases a distance-independent diffusion constant. In the case of free diffusion holds $\mathcal{R}(r) = D^{-1}r^{-2}$ and, hence,

$$\int_{R_o}^\infty dr\, \mathcal{R}(r) = 1/DR_o. \quad (20)$$

From this results

$$k(R_o, w) = \frac{4\pi DR_o}{1 + D/R_o w}. \quad (21)$$

In the case of very effective reactions, i.e., for very large w, this becomes

$$k(R_o, w) = 4\pi\, DR_o, \quad (22)$$

which is the well-known rate constant for diffusion-controlled reaction processes. In the case of a Coulomb interaction between Glu^- and CD, one obtains

$$\int_{R_o}^\infty dr\, \mathcal{R}(r) = \frac{1}{D}\int_{R_o}^\infty dr\frac{1}{r^2}\exp\left[\frac{\beta q_{CD}\, q_S}{\epsilon r}\right] = \frac{1}{R_L D}\left(e^{R_L/R_o} - 1\right), \quad (23)$$

where

$$R_L = \beta q_{CD}\, q_S/\epsilon \quad (24)$$

defines the so-called Onsager radius. Note that R_L can be positive or negative, depending on the sign of $q_{CD}\, q_S$, but that the integral over $\mathcal{R}(r)$ (Eq. 23) is always positive. The rate constant derived in Eq. 16 can then be written as

$$k(R_o, w) = \frac{4\pi DR_L}{\left(R_L D/R_o^2 w\right)e^{R_L/R_o} + e^{R_L/R_o} - 1}. \quad (25)$$

Quantum yield of diffusion-controlled reaction

One can express the rate constants derived above in the form

$$k(R, w) = k(R', \infty)\phi(R', R, w), \quad (26)$$

where, according to the definition above, $k(R', \infty)$ is the rate constant for the case that every encounter at R' leads to a reaction and where $\phi(R', R, w)$ is then the probability, referred to as the quantum yield, that for a finite w the reaction actually occurs at R when diffusion started at R'. From Eq. 16 follows

$$\phi(R', R, w) = \frac{\int_{R'}^\infty dr\, \mathcal{R}(r)}{\left(e^{\beta U(R)}/R^2 w\right) + \int_R^\infty dr\, \mathcal{R}(r)}. \quad (27)$$

In the case of free diffusion and when $R' = R$ holds, using Eq. 20, we obtain

$$\phi(R' = R, R, w) = \frac{1}{D/Rw + 1}. \quad (28)$$

RESULTS

MscS furnishes a cell's initial defense against cell lysis, being gated at low osmotic pressure differences, namely, of a few tens mmHg. At this low pressure point, i.e., without threat of imminent lysis, the cell may protect itself while preventing cell depolarization and loss of particularly

valuable osmolytes, employing for this purpose the cytoplasmic domain (CD) as a filter.

One such osmolyte should be the Glu^- ion, the main negative counter charge for the cell's positive ions like K^+ and also an essential metabolite. In this section we investigate, hence, the role of the CD as a filter that controls Glu^- and K^+ efflux. This can be achieved by the CD acting as what we like to refer to as an entropic filter that prevents Glu^- from reaching the CD pores, but once Glu^- enters a pore, lets it pass unhindered due to favorable enthalpic interactions to prevent unclogging of the pores. We note that the cell potential of ~ -100 mV tends to expel Glu^- from the cell and retain K^+. The CD can act by slowing efflux of Glu^-, while attracting K^+, achieving thereby a neutral osmolyte current and conserving partially the cellular potential along with retaining as much as possible the valuable Glu^- ion.

In the following we demonstrate theoretically and computationally CD's action as such entropic filter. We first describe mathematically the diffusion-controlled approach of Glu^- to the CD and its side opening entrance (see Fig. 1 *d* and Movie S1 and Movie S2). We then demonstrate that Glu^- can readily pass the pores by computing Glu^-'s potential of mean force in the pores and then calculating on this basis the mean time of passage through the pore (see Fig. 1 *d*). Our conclusions regarding CD's function can be based on a solely qualitative treatment of the overall translocation behavior of Glu^-, as the filter effect of the CD turns out to be quite drastic.

Electrostatic potential

The first step in Glu^- translocation involves the diffusive approach to the CD and Glu^- entering one of CD's pores, in the following referred to as the "openings." As Glu^- carries a $-e$ charge it experiences a repulsive, long-range interaction with the $-7e$ overall charge of the CD, screened by the water dielectric property. Fig. 2 shows the electrostatic potential inside and outside of the CD averaged over a molecular dynamics (MD) trajectory as described in Methods. The potential is weakly repulsive for Glu^- outside and inside the CD, in particular in the vicinity of the side openings whereas the inaccessible protein part is attractive.

Diffusion of Glu^- and K^+ to cytoplasmic domain and its openings

A mathematical description of the diffusive approach for the realistic geometry and potential of the CD shown in Fig. 2 requires a numerical approach which would not be very illuminating at this point, but should be furnished eventually. For the sake of qualitative argument, a simplification to a radially symmetric geometry and potential, that permits an analytical treatment, is sufficient and will be pursued now. For this purpose we employ the stationary rate constant of the diffusion-controlled binding to the CD opening, $k(R_o, w)$, as

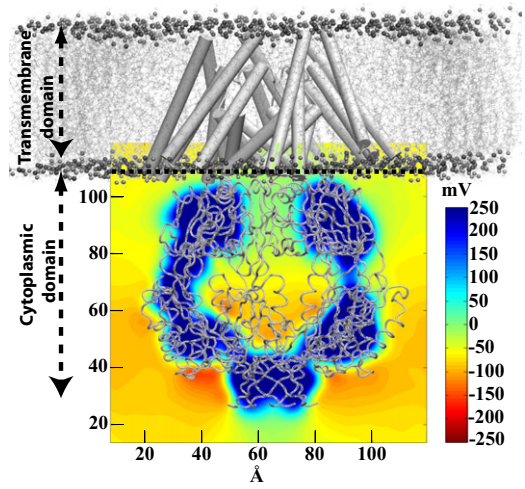

FIGURE 2 Time-averaged electrostatic potential due to the MscS cytoplasmic domain. The potential shown has been determined through averaging over our all-atom MD simulations as described in Aksimentiev and Schulten (30). The transmembrane domain of MscS, shown in shading as an overlay over a standard membrane, has not been included in the calculation. The potential has been obtained under zero biasing potential. The structure of the cytoplasmic MscS domain is superimposed to facilitate the interpretation of the electrostatic features shown.

derived in Methods for the case of a Coulomb potential (see Eq. 25). In the case of the potential $U(r) = q_{CD}q_{Glu}/\varepsilon r$ with $q_{CD} = -7e$, $q_{Glu} = -e$, and $\varepsilon = 80$ (approximate relative dielectric constant of water), one determines for $R_L = 7\beta e^2/\varepsilon$ the value $R_L = 49$ Å. The radius of the CD at the level of the side openings is $R_o = 43$ Å (as measured using VMD). We assume for the diffusion constant an r-independent value of $D_{Glu} = 0.75 \times 10^{11}$ Å^2/s (44). To determine $k(R_o, w)$, one needs to specify the reaction constant w accounting for the probability, once Glu^- has encountered the CD surface, that the ion actually enters an opening.

To estimate w for the case of a CD surface dotted with seven openings we envision the following process: when Glu^- has approached the CD surface it diffuses around until it hits the mouth of a CD opening (see Fig. 1 *c*) and then enters the opening. The probability of this to happen is the quantum yield $Q(R, R, w)$ of a diffusion process starting at the surface of the CD and being absorbed by an opening, i.e., for $R = R_o$. Because the electrostatic potential near the surface of the CD is largely negative, as seen in Fig. 2, we assume that openings are entered only for more or less direct hits, such that we choose w through the condition

$$Q(R, R, w) = q_o, \tag{29}$$

where $q_o = 7r_o^2/4R_o^2$ is the ratio of the combined area of seven openings, i.e., of $7 \times \pi r_o^2$, to the total CD surface, i.e., $4\pi R_o^2$. Using $r_o = 4.5$ Å (this value will be rationalized below) and $R_o = 43$ Å, we estimate $q_o \approx 0.02$. We derived in Methods the expression Eq. 28 for $Q(R, R, w)$, which can be written as

$$Q(R,R,w) = 1 - \frac{D}{w\,R + D}. \quad (30)$$

From this follows the desired expression for w, namely,

$$w = \frac{q_o}{1-q_o}\frac{D}{R}. \quad (31)$$

Rewriting the last result as $D/wR = (1 - q_o)/q_o$, one can express Eq. 25 as

$$k(R_o,w) = 4\pi\, D\, R_{\rm L}\left[\frac{R_{\rm L}}{R_o}\frac{1-q_o}{q_o}e^{R_{\rm L}/R_o} + e^{R_{\rm L}/R_o} - 1\right]^{-1}. \quad (32)$$

For $R_o = 43$ Å, the term $\exp(R_L/R_o) - 1 = 2.12$ is of order 1, i.e., is much smaller than the term $(R_L/R_o)[(1 - q_o)/q_o]\exp(R_L/R_o)$, which for the present value of q_o is of order 100 and, hence, $\exp(R_L/R_o) - 1$ can be neglected, leaving one with the expression

$$k(R_o,w) = 4\pi\, D\, R_o\frac{q_o}{1-q_o}e^{-R_{\rm L}/R_o}. \quad (33)$$

Approximating $\exp(-R_L/R_o) \approx 1$ and $1 - q_o \approx 1$, one obtains the rate constant $k = 4\pi DR_oq_o$, i.e., the diffusion-controlled rate constant reduced by the factor q_o (for comparison, see Eq. 22). This is the expected result in the case of weak Coulomb repulsion and a small reaction probability.

We conclude from the mathematical description provided that the approach of Glu^- to the CD is governed roughly by the rate constant stated in Eq. 33. The factor $4\pi DR_o$ describes the rate constant for diffusion toward the CD (radius R_o), the factor $q_o/(1 - q_o)$ accounts for the time delay due to the small size of the CD openings, and the Boltzmann factor $\exp(-R_L/R_o)$ includes the effect of the electrostatic repulsion between Glu^- and the CD. Employing the already stated numerical values for R_o and R_L along with the stated diffusion coefficient $D_{\rm Glu}$ and a concentration $c_{\rm Glu} = 0.2$ mol/L (28), one obtains for the time τ_1 of diffusion-controlled entering of the CD openings by Glu^-

$$\tau_1 = 1/k(R_o,w)c_{\rm Glu} \approx 32 \text{ ns}, \quad (34)$$

i.e., on average, approximately one Glu^- per 32 ns enters a CD opening.

If the entire CD would be porous for Glu^-, the average time τ_1 of reaching the pores would be 0.6 ns, i.e., 50 times shorter than without the filter function of the CD openings. Clearly, the CD acts as an entropic filter, turning randomly a large fraction of approaching Glu^- away, preventing, thereby, a quick loss of Glu^-.

For K^+ the electrostatic potential around the CD is attractive. One can assume that, once the ion has reached the CD surface, the quantum yield of finding a pore opening is close to one as K^+ remains attracted to the surface long enough to eventually find an opening. The rate of K^+ entering the CD openings is then given by Eqs. 24 and 25 for $w \to \infty$ and $q_s = e$, i.e., $R_L = -49$ Å, which is $4\pi D_{\rm K}|R_L|c_{\rm K}/(1 - \exp(-|R_L/R_o|))$; here we assume that the search time of K^+ on the CD surface is negligible. With $D_{\rm K} = 2 \times 10^{11}$ Å^2/s (45), $c_{\rm K} = 0.2$ mol/L, and for $|R_L/R_o| = 1.139$, one obtains $\tau_1 = 0.045$ ns. To this time should be added the search time, $\tau_{\rm search}$, of a few nanoseconds. Even though $\tau_{\rm search}$ is larger than τ_1, the added contribution does not matter, as we will see below.

Free energy of Glu^- and K^+ translocation

The entropic filter mechanism of the CD is based on the premise that CD wall openings do not get clogged by substances like Glu^-, i.e., that the passage (through the CD openings) time of Glu^-, τ_2, is very short compared to the open-time of MscS. The value τ_2 is estimated computationally in the next section.

The free energy profile characterizing Glu^- translocation through the side openings, calculated as described in Methods, is shown in Fig. 3. The profile shows Glu^-, initially at a distance 51 Å away from the center of the CD, moving toward the entrance of the opening subject to a slightly attractive potential due to interaction with positively charged residues, lysines and arginines, that line the walls of the openings. The openings establish a barrier of only ~2 kcal/mol for the translocation of Glu^- which is sufficiently low to prevent Glu^- from clogging the opening. It is important to note that throughout the 0.38 μs of ABF simulations, the opening remained quite stable with only minute fluctuations in structure detected. The distance RMSD computed for the backbone of residues lining the opening never exceeded 1.45 Å. We note that the harmonic restraints applied to the C_α atoms of residues 274 and 120 in subunits P1–P7 (see Methods) should not affect the stated RMSD values because residues 274 and 120 are far away from the side openings. Once Glu^- enters the CD interior, it experiences mainly unfavorable Coulomb interactions of 0.5 kcal/mol; this slightly unfavorable interaction is also discernable in Fig. 3 as well as in the electrostatic potential Fig. 2.

We note from Fig. 3 that from the cytoplasmic direction, a first barrier arises inside the side opening at $\zeta = 20$ Å; Fig. 3 *d* shows that at this ζ-value, the opening has a radius of 4.5 Å, which is why we assumed in our calculation of $k(R_o,w)$ above this as the r_o value.

The small barrier for Glu^- ion suggests τ_2 for Glu^- ion to be small such that these ions may readily pass through the openings. This is consistent with spontaneous diffusion of Glu^- ions passing through the side openings of CD; such diffusion was observed during our simulations. Indeed, during 0.38 μs, four events of spontaneous diffusion of Glu^- ions were observed. In one of the four cases, a Glu^- ion transited from the bulk to the CD interior, whereas, in other cases, the ions moved out of the CD. We also observed spontaneous transit of a K^+ ion moving from bulk to the interior of the CD. Spontaneous diffusion of K^+ and Cl^-

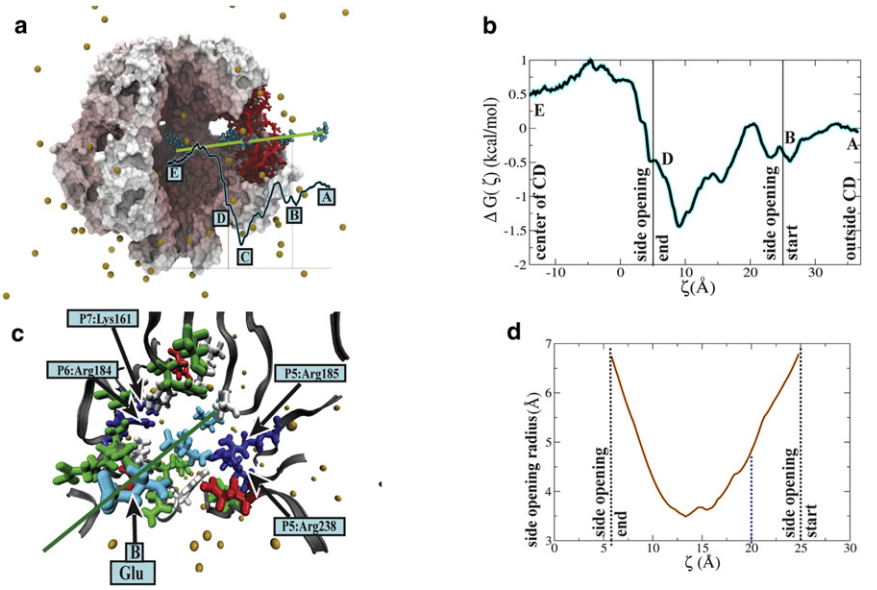

FIGURE 3 Free energy profile for Glu^-, a key cellular osmolyte, translocating a side opening in the MscS cytoplasmic domain. (*a*) View of the outside and inside of the cytoplasmic domain, cut open. The protein is shown in surface representation. On the right, an opening is presented with the protein shown in red in ribbon representation with external side groups in licorice representation. Ions (K^+) are shown as gold spheres; water is not shown. Glu^- is shown in five stages of translocation, labeled *A*, *B*, *C*, *D*, and *E*. The potential of mean force, accounting for the energy of Glu^- during translocation and obtained from an equilibrium ABF simulation totaling 0.38 μs of sampling, is shown below the Glu^- snapshots; the potential has been determined along the line connecting the Glu^- snapshots which are also denoted in the potential. (*b*) Potential of mean force for translocating Glu^-. The potential of mean force in panel *a* is shown again with fully labeled axes. The domain side opening is ~20 Å long; the distance from the inside end of the opening and the domain center is ~20 Å with the center of CD corresponding to −14 Å on the ζ-axis; the potential of mean force varies over a range of 2 kcal/mol, i.e., only by 4 k_BT. (*c*) Close-up view of MscS amino-acid side groups lining the domain opening. The residues coming within 4 Å of Glu^- along the translocation pathway are depicted in licorice representation in white, green, red, and blue for nonpolar, polar, negative, and positive amino-acid side groups, respectively; the protein distant from the opening is shown in dark gray ribbon representation; K^+ ions are shown in gold. The Glu^- ion, shown at locations *B*–*D* (compare to panels *a* and *b*) is colored in light blue. The green line shown passing through the Glu^- snapshots corresponds to the ζ-axis in panel *b*. Glu^- position C corresponds to an enthalpic energy minimum where the ion is stabilized by interactions with Lys^{161} of subunit P7, Arg^{184} of subunit P6, and with Arg^{238} and Arg^{185} of subunit P5. Movie S2 provides a view of Glu^- moving through a CD opening and interacting with side groups lining the opening. (*d*) Size of the openings in the MscS cytoplasmic domain. The graph shows the radius profile of the side opening as determined by the program HOLE (50); the radius is smallest at the center of the opening (compare to panel *b*); the opening stretches from 5 Å to 25 Å.

ions through the side opening were also reported in earlier studies (13,15). These observations suggest that the free energy barrier for K^+ is as small as for the Glu^- ion, allowing unhindered permeation of K^+ ions via the openings. Using free-energy perturbation (see the Supporting Material), replacing Glu^- by a K^+, at positions *A*, *C*, and *E* (Fig. 3, *a* and *b*) along the translocation pathway, the barrier at the opening was estimated to be ~3.1 kcal/mol. These observations also suggest that the passage times τ_2 for Glu^- and K^+ ions are comparable.

Mean passage time τ_2 of Glu^- and K^+ passing through a CD opening

To further illustrate that Glu^- can readily pass through with only a short residence time inside the CD openings, we evaluate the mean passage time, τ_2, from the obtained PMF, $U(x)$, according to (46,47)

$$\tau_2 = \frac{1}{D}\int_{x_1}^{x_0} dx\, e^{\beta U(x)} \int_{x}^{x_0} dy\, e^{-\beta U(y)}. \qquad (35)$$

Here, we assume the same diffusion coefficient of glutamate in water as above, i.e., $D_{Glu} = 0.75 \times 10^{11}$ Å^2/s. The integration limits x_1 and x_0 correspond to Glu^- set at an initial position outside the CD, x_1, and reaching the center of the CD, x_0 (see Fig. 3 *b*). Numerical integration of the above expression yields τ_2 ~40 ns. MscS channel open times from patch-clamp measurements are ~100 ms (12); τ_2 is extremely short in comparison such that one can conclude the CD openings to remain unclogged.

To obtain the corresponding value of τ_2 for K^+, Eq. 35 was numerically integrated after splining over $U(x)$ obtained at three positions, namely, *A*, *C*, and *E* (Fig. 3, *a* and *b*), and estimated from free-energy perturbation calculations as described in Methods (see also Supporting Material). Here, the same integration limits x_1 and x_0 were used as for Glu^-. Assuming for the K^+ ion a diffusion coefficient $D_K = 2.0 \times 10^{11}$ Å^2/s, τ_2 for K^+ ion is ≈20 ns. The stated τ_2 values for Glu^- and K^+ suggest that both ions permeate the CD openings quickly.

Mixing of ions

The simulated CD contains ~2600 water molecules. At the molar concentration of 56 mol/L, the water molecules occupy ~8×10^4 Å^3 and in equilibrium with Glu^- and K^+ concentrations of 0.2 mol/L, should harbor ~10 ions of each type delivered with a time constant of $\tau' = \tau_1 + \tau_2$ where τ_1 and τ_2, already discussed, are given in Table 1. We derive in the Supporting Material that the ions in a spherical cavity prefer, energetically, an equal number of positive and negative ions due to Coulomb interaction; for a cavity the size of the CD, a balanced state is being favored by several k_BT. We conclude that the CD maintains, on average, a state of

TABLE 1 Computed mean passage times τ_1, τ_2, τ_3, and τ_3' for Glu^- and K^+ ions

Ion	τ_1 (ns)	τ_2 (ns)	τ_3 (ns)	τ_3' (ns)	$\tau = \tau_1 + \tau_2 + \tau_3$ (ns)
Glu^-	32	40	10	260	82
K^+	0.045	20	35	375	55

Value τ_3 is the mean first-passage time through the actual transmembrane channel (see text); τ_3' is the mean first-passage time from the center of the CD through the transmembrane channel.

~10 Glu^- and 10 K^+ ions. The ions spread diffusively throughout the CD interior such that there are always some ions near the membrane channel exit. The scenario suggested depends critically on the entrance times τ' for the ions being short compared to their exit times τ_3 being evaluated now. According to Table 1, the entrance time is 72 ns for Glu^- and 20 ns for K^+.

Times τ_3 of Glu^- and K^+ exiting through transmembrane channel

The exit times τ_3 can be estimated as mean first-passage times of the ions permeating from inside the CD to the extracellular space, assuming the open state conformation of MscS (PDB:2VV5) (11). The value τ_3 can be evaluated for a passage governed by an effective potential, $\tilde{U}(x)$, and then is given by the expression (see the Supporting Material)

$$\tau_3 = \int_{x_{\text{center}}}^{x_{\text{out}}} dx\, D^{-1}(x) \exp\left[\beta\tilde{U}(x)\right] \int_{x_{\text{apex}}}^{x} dx' \exp\left[-\beta\tilde{U}(x')\right]. \tag{36}$$

In the above expression, $\tilde{U}(x) = U(x) - k_B T \ln Z(x)$ combines enthalpic $[U(x)]$ and entropic $[-k_B T \ln Z(x)]$ contributions. $U(x)$ is the transmembrane potential characterized through the resting potential of the *E. coli* cell, namely, $V_o = -100$ mV (48,49); $Z(x)$ accounts for the CD geometry along the conduction path CD $\rightarrow$ channel and is $Z(x) = \pi(r^2(x)/r_0{}^2)$, where $r(x)$ is the radius of the cross section along the symmetry axis, x, of the MscS and r_0 is a reference radius, the value of which drops out of the evaluation. The HOLE program (50) was used to determine the radius profile of MscS and, thus, $Z(x)$. In Eq. 36, x_{apex}, x_{center}, and x_{out} are positions along the CD axis located at the CD apex, CD center, and end-point of the transmembrane channel. We note that the integration limit x_{apex} in Eq. 36 accounts for the possibility that an ion diffuses in the direction away from the channel mouth before it exits the CD.

$Z(x)$ accounts for an effective entropic barrier arising from the need that the diffusing ions have to find the channel mouth. In case of well-mixed ions of sufficient density, one can assume that there are always Glu^- and K^+ ions near the mouth such that little time may need to be spent to find it. To estimate the time to exit the CD, one can determine τ_3 for two scenarios, 1), starting near the channel mouth (in which case x_{apex} and x_{center} in Eq. 36 are replaced by x_{exit}), and 2), starting from the center, with $Z(x)$ included.

Table 1 lists for the two scenarios the times 10 ns and 260 ns in the case of Glu^-, and 35 ns and 375 ns for K^+. Comparing these times with the entrance times, τ' , discussed above we conclude that the times to search and exit the CD, τ_3', are significantly longer than the entrance times whereas the pure exit times, τ_3, are shorter in the case of Glu^- and longer in the case of K^+. We conclude then that the CD, in mixing the ions, keeps always some Glu^- and K^+ ions ready near the channel mouth, to exit faster than a new ion could that had just permeated a CD side pore.

We compare finally scenario 1) exit times, τ_3, with the ion conductances measured for the respective ions. The 10-ns value for Glu^- corresponds to a current of 100×10^6 ions/s or a channel conductance of $\approx$230 pS. Because an open MscS channel can accommodate two Glu^- ions at any one time, the channel conductance for Glu^- increases by a factor of two and should then be ~500 pS, which is in agreement with the experimentally measured channel conductance for Glu^- (2). This agreement is an argument in favor of the scenario described for the overall ion conduction of MscS in which the CD provides an ion buffer that effectively accelerates ion permeation as mixed ions search for the channel mouth in parallel, rather than sequentially.

Taken together, the total passage time (see Table 1), $\tau = \tau_1 + \tau_2 + \tau_3$, is nearly the same for the two ions, irrespective of the time τ_{search} (discussed above), which should only be a few nanoseconds. The values suggest that the CD serves to maintain an overall balance between positively and negatively charged osmolytes leaving the cell, precluding loss of cell polarization. The overall balance of osmolytes is also enforced by electrostatic interaction between osmolytes inside the CD.

DISCUSSION

The cytoplasmic domain (CD) is a conspicuous component of the mechanosensitive channel, MscS. It is not directly involved in the protein's TM channel. Yet, it makes up the major body of the protein. Given the CD's sievelike and mixing bowl-like architecture along with its cytoplasmic position, a filter and mixer function suggests itself and has been investigated in this study.

The filter function is more complex than one realizes right away, the key problem arising from the need to avoid clogging the filter. A naive solution regarding the filter mechanism would be to involve in the filter openings an enthalpic barrier to solutes. However, this would be the worst solution because it would promote clogging. In fact, the opposite solution is more advisable, namely, that valuable solutes pass openings quickly, but that they do not reach the openings in the first place. We call this an entropic filter mechanism.

In our study we have identified indeed such property for the CD openings of MscS. We focused first on Glu^-, a key osmolyte and metabolite in *E. coli*, present at high concentration. We find that Glu^- passes the CD openings readily

without significant enthalpic barrier, which suggests that the CD acts as an entropic filter. The average electrostatic field around the CD supports this notion, because the CD surface potential is repulsive in the case of the negative Glu^- osmolyte. We provide in our study a formal description of the entropic filter function employing the theory of diffusion-controlled reaction processes. Clogging of the CD openings is investigated through calculation of the mean first-passage time τ_2 of Glu^- making it through the channel, which was determined from a potential of mean force obtained through simulation: τ_2 turned out to be much shorter than typical "open" times of MscS, which implies that the CD openings remain basically unclogged as regards Glu^-. We then calculated the mean passage time for Glu^- to leave the CD and reach the extracellular space. The total time $\tau = \tau_1 + \tau_2 + \tau_3$ is estimated to be ~80 ns.

We then focused on K^+, also present at high concentration in *E. coli* cells. In this case, the overall exit time τ is ~55 ns, i.e., close to the 80 ns Glu^- value, but τ_1 is shorter and τ_3 is longer than for Glu^-. Based on these times for Glu^- and K^+, we conclude the filter function of the CD shown in Fig. 4. MscS, through the combination of CD and channel, manages an amazing feat, namely even though the cell potential by itself clearly favors expulsion of Glu^-, compensation through a short K^+ τ_1 makes the overall exit times of Glu^- and K^+ about the same. This impressive balance is likely stabilized through electrostatic interactions in the CD. The size of the CD with an inside opening of volume 8×10^4 Å^3 permits that at any one time ~10 positive and ~10 negative ions are being harbored, given the cytoplasmic ion concentration of 0.2 mol/L. The lowest electrostatic energy is assumed when the CD harbors the same number of positive and negative ions, thereby favoring a neutral osmolyte current through MscS in the open state.

Our study is but a first step into the filter and mixing function of the MscS CD. Given the many types of solutes that need to be considered in this regard, the study needs to be extended, though for a first investigation it seemed wise to concentrate on just two ions, Glu^- and K^+. Future studies should involve a multiscale approach that combines transport theory with MD simulations, finite element method of the bulk cytosol with the detailed geometry of MscS CD and membrane surface, and covers the entire solute translocation, i.e., from cytoplasm to the extracellular space, as a nonstationary process. A particularly exciting aspect of future studies should be ion-ion interaction effects in the CD that favor neutral efflux and preserve cell polarity.

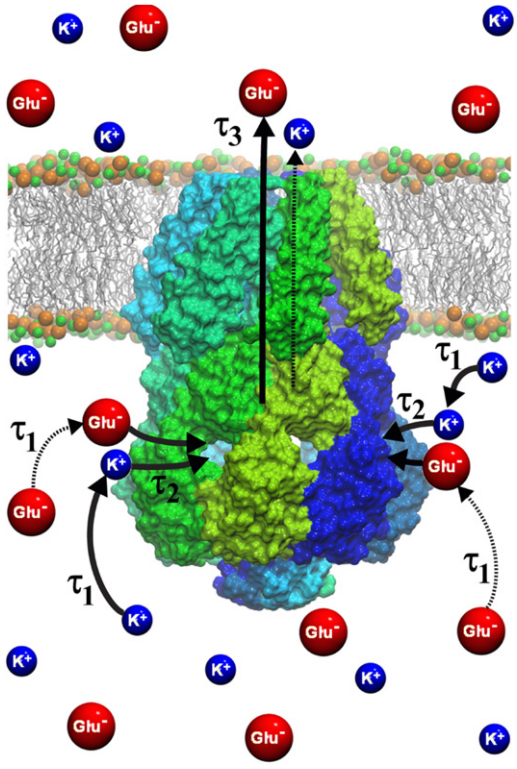

FIGURE 4 Diffusion of Glu^- and K^+ ions through the cytoplasmic domain of MscS. Due to the topology of the electrostatic potential in conjunction with the intrinsic characteristics of the osmolytes, K^+ ions diffuse faster than Glu^- ions toward the CD (τ_1). They permeate through the pores at comparable times (τ_2), but exit the channel slower than their anionic counterpart (τ_3) (fast translocation shown as *thick*, *solid arrows* and slow one as *thin*, *dashed arrows*).

SUPPORTING MATERIAL

Four figures, additional information with equations, and two movies are available at http://www.biophysj.org/biophysj/supplemental/S0006-3495(11)00612-6.

All-atom MD simulations discussed here were performed using the package NAMD (31). Molecular images in this article were rendered using the molecular visualization software VMD (27).

M.S. is a Howard Hughes Medical Institute Fellow of the Helen Hay Whitney Foundation. This work was supported by grants from the National Institutes of Health (1 R01-GM067887). Computer time was provided by the National Center for Supercomputing Applications and the Texas Advanced Computing Center via Large Resources Allocation Committee grant MCA93S028.

REFERENCES

1. Hamill, O. P., and B. Martinac. 2001. Molecular basis of mechanotransduction in living cells. *Physiol. Rev.* 81:685–740.
2. Martinac, B., M. Buechner, …, C. Kung. 1987. Pressure-sensitive ion channel in *Escherichia coli*. *Proc. Natl. Acad. Sci. USA.* 84: 2297–2301.
3. Levina, N., S. Tötemeyer, …, I. R. Booth. 1999. Protection of *Escherichia coli* cells against extreme turgor by activation of MscS and MscL mechanosensitive channels: identification of genes required for MscS activity. *EMBO J.* 18:1730–1737.
4. Berrier, C., A. Coulombe, …, A. Ghazi. 1989. A patch-clamp study of ion channels of inner and outer membranes and of contact zones of *E. coli*, fused into giant liposomes. Pressure-activated channels are localized in the inner membrane. *FEBS Lett.* 259:27–32.
5. Berrier, C., M. Besnard, …, A. Ghazi. 1996. Multiple mechanosensitive ion channels from *Escherichia coli*, activated at different thresholds of applied pressure. *J. Membr. Biol.* 151:175–187.

6. Sukharev, S. I., W. J. Sigurdson, …, F. Sachs. 1999. Energetic and spatial parameters for gating of the bacterial large conductance mechanosensitive channel, MscL. *J. Gen. Physiol.* 113:525–540.
7. Ajouz, B., C. Berrier, …, A. Ghazi. 1998. Release of thioredoxin via the mechanosensitive channel MscL during osmotic downshock of *Escherichia coli* cells. *J. Biol. Chem.* 273:26670–26674.
8. Berrier, C., A. Garrigues, …, A. Ghazi. 2000. Elongation factor Tu and DnaK are transferred from the cytoplasm to the periplasm of *Escherichia coli* during osmotic downshock presumably via the mechanosensitive channel MscL. *J. Bacteriol.* 182:248–251.
9. Bass, R. B., P. Strop, …, D. C. Rees. 2002. Crystal structure of *Escherichia coli* MscS, a voltage-modulated and mechanosensitive channel. *Science.* 298:1582–1587.
10. Steinbacher, S., R. B. Bass, …, D. C. Rees. 2007. Structures of the prokaryotic mechanosensitive channels MscL and MscS. *In* Current Topics in Membranes in Mechanosensitive Ion Channels, Part A, *Vol. 58*. O. P. Hamill, editor. Elsevier, New York, NY. 1–24.
11. Wang, W., S. S. Black, …, I. R. Booth. 2008. The structure of an open form of an *E. coli* mechanosensitive channel at 3.45 Å resolution. *Science.* 321:1179–1183.
12. Edwards, M. D., Y. Li, …, I. R. Booth. 2005. Pivotal role of the glycine-rich TM3 helix in gating the MscS mechanosensitive channel. *Nat. Struct. Mol. Biol.* 12:113–119.
13. Sotomayor, M., and K. Schulten. 2004. Molecular dynamics study of gating in the mechanosensitive channel of small conductance MscS. *Biophys. J.* 87:3050–3065.
14. Sotomayor, M., T. A. van der Straaten, …, K. Schulten. 2006. Electrostatic properties of the mechanosensitive channel of small conductance MscS. *Biophys. J.* 90:3496–3510.
15. Vora, T., B. Corry, and S.-H. Chung. 2006. Brownian dynamics investigation into the conductance state of the MscS channel crystal structure. *Biochim. Biophys. Acta.* 1758:730–737.
16. Spronk, S. A., D. E. Elmore, and D. A. Dougherty. 2006. Voltage-dependent hydration and conduction properties of the hydrophobic pore of the mechanosensitive channel of small conductance. *Biophys. J.* 90: 3555–3569.
17. Sotomayor, M., V. Vásquez, …, K. Schulten. 2007. Ion conduction through MscS as determined by electrophysiology and simulation. *Biophys. J.* 92:886–902.
18. Akitake, B., A. Anishkin, …, S. Sukharev. 2007. Straightening and sequential buckling of the pore-lining helices define the gating cycle of MscS. *Nat. Struct. Mol. Biol.* 14:1141–1149.
19. Vásquez, V., M. Sotomayor, …, E. Perozo. 2008. Three-dimensional architecture of membrane-embedded MscS in the closed conformation. *J. Mol. Biol.* 378:55–70.
20. Vásquez, V., M. Sotomayor, …, E. Perozo. 2008. A structural mechanism for MscS gating in lipid bilayers. *Science.* 321:1210–1214.
21. Koprowski, P., and A. Kubalski. 2003. C termini of the *Escherichia coli* mechanosensitive ion channel (MscS) move apart upon the channel opening. *J. Biol. Chem.* 278:11237–11245.
22. Miller, S., W. Bartlett, …, I. R. Booth. 2003. Domain organization of the MscS mechanosensitive channel of *Escherichia coli*. *EMBO J.* 22:36–46.
23. Miller, S., M. D. Edwards, …, I. R. Booth. 2003. The closed structure of the MscS mechanosensitive channel. Cross-linking of single cysteine mutants. *J. Biol. Chem.* 278:32246–32250.
24. Nomura, T., M. Sokabe, and K. Yoshimura. 2008. Interaction between the cytoplasmic and transmembrane domains of the mechanosensitive channel MscS. *Biophys. J.* 94:1638–1645.
25. Machiyama, H., H. Tatsumi, and M. Sokabe. 2009. Structural changes in the cytoplasmic domain of the mechanosensitive channel MscS during opening. *Biophys. J.* 97:1048–1057.
26. Schumann, U., M. D. Edwards, …, I. R. Booth. 2004. The conserved carboxy-terminus of the MscS mechanosensitive channel is not essential but increases stability and activity. *FEBS Lett.* 572:233–237.
27. Humphrey, W., A. Dalke, and K. Schulten. 1996. VMD: visual molecular dynamics. *J. Mol. Graph.* 14:33–38, 27–28.
28. Leirmo, S., C. Harrison, …, M. T. Record, Jr. 1987. Replacement of potassium chloride by potassium glutamate dramatically enhances protein-DNA interactions in vitro. *Biochemistry.* 26:2095–2101.
29. Essmann, U., L. Perera, …, L. G. Pedersen. 1995. A smooth particle mesh Ewald method. *J. Chem. Phys.* 103:8577–8593.
30. Aksimentiev, A., and K. Schulten. 2005. Imaging α-hemolysin with molecular dynamics: ionic conductance, osmotic permeability, and the electrostatic potential map. *Biophys. J.* 88:3745–3761.
31. Phillips, J. C., R. Braun, …, K. Schulten. 2005. Scalable molecular dynamics with NAMD. *J. Comput. Chem.* 26:1781–1802.
32. Darve, E., and A. Pohorille. 2001. Calculating free energies using average force. *J. Chem. Phys.* 115:9169–9183.
33. Darve, E., D. Wilson, and A. Pohorille. 2002. Calculating free energies using a scaled-force molecular dynamics algorithm. *Mol. Simul.* 28:113–144.
34. Hénin, J., and C. Chipot. 2004. Overcoming free energy barriers using unconstrained molecular dynamics simulations. *J. Chem. Phys.* 121: 2904–2914.
35. Hénin, J., K. Schulten, and C. Chipot. 2006. Conformational equilibrium in alanine-rich peptides probed by reversible stretching simulations. *J. Phys. Chem. B.* 110:16718–16723.
36. Chipot, C., and A. Pohorille. 2007. Free Energy Calculations. Theory and Applications in Chemistry and Biology. Springer-Verlag, Berlin, Germany.
37. Hénin, J., A. Pohorille, and C. Chipot. 2005. Insights into the recognition and association of transmembrane α-helices. The free energy of α-helix dimerization in glycophorin A. *J. Am. Chem. Soc.* 127:8478–8484.
38. Hénin, J., E. Tajkhorshid, …, C. Chipot. 2008. Diffusion of glycerol through *Escherichia coli* aquaglyceroporin GlpF. *Biophys. J.* 94: 832–839.
39. Chipot, C., and K. Schulten. 2008. Understanding structure and function of membrane proteins using free energy calculations. *In* Biophysical Analysis of Membrane Proteins. Investigating Structure and Function. E. Pebay-Peyroula, editor. Wiley, Weinheim, Germany. 187–211.
40. Schulten, Z., and K. Schulten. 1977. The generation, diffusion, spin motion, and recombination of radical pairs in solution in the nanosecond time domain. *J. Chem. Phys.* 66:4616–4634.
41. Debye, P. 1942. Reaction rates in ionic solutions. *Trans. Electrochem. Soc.* 82:265–272.
42. Eigen, M. 1954. Kinetics of high-speed ion reactions in aqueous solution. *Z. Phys. Chem.* 1:176–200.
43. Gardiner, C. W. 1983. Handbook of Stochastic Methods. Springer, New York.
44. Zheng, K., A. Scimemi, and D. A. Rusakov. 2008. Receptor actions of synaptically released glutamate: the role of transporters on the scale from nanometers to microns. *Biophys. J.* 95:4584–4596.
45. Hille, B. 1992. Ionic Channels of Excitable Membranes, 2nd Ed. Sinauer Associates, Sunderland, MA.
46. Szabo, A., K. Schulten, and Z. Schulten. 1980. First passage time approach to diffusion controlled reactions. *J. Chem. Phys.* 72:4350–4357.
47. Schulten, K., Z. Schulten, and A. Szabo. 1981. Dynamics of reactions involving diffusive barrier crossing. *J. Chem. Phys.* 74:4426–4432.
48. Foster, J. W. 2004. *Escherichia coli* acid resistance: tales of an amateur acidophile. *Nat. Rev. Microbiol.* 2:898–907.
49. Felle, H., J. S. Porter, …, H. R. Kaback. 1980. Quantitative measurements of membrane potential in *Escherichia coli*. *Biochemistry.* 19:3585–3590.
50. Smart, O. S., J. M. Goodfellow, and B. A. Wallace. 1993. The pore dimensions of gramicidin A. *Biophys. J.* 65:2455–2460.